Optics Communications 531 (2023) 129233

Contents lists available at ScienceDirect

Optics Communications

journal homepage: www.elsevier.com/locate/optcom

All-fiber acetylene-referenced optical frequency comb

Yongqi Li [a], Xiaohong Hu [b], Haihao Cheng [b], Yishan Wang [b], Yanzhao Yang [c], Shun Wu [a,*]

[a] Hubei Key Laboratory of Optical Information and Pattern Recognition, Wuhan Institute of Technology, Wuhan 430205, China
[b] State Key Laboratory of Transient Optics and Photonics, Xi'an Institute of Optics and Precision Mechanics, Chinese Academy of Sciences, Xi'an 710119, China
[c] China Electronics Technology Group 41st Research Institute, Qingdao 266555, China

ARTICLE INFO

Keywords:
Mode-locked fiber
Optical frequency comb
Frequency stabilization
Optical reference

ABSTRACT

We demonstrated an all-fiber compact Erbium-doped optical frequency comb based on optical reference. Compared with the traditional RF reference, the whole system adopts the all-fiber design of optical reference. Comb stabilization is achieved by simultaneously locking the repetition rate (f_r) to an RF reference and an optical comb tooth to a CW reference. The standard deviation of the f_r frequency in 4.5 hours was recorded as 0.37 mHz, leading to a fraction instability of 4.3 $\times 10^{-12}$ at 1 s gate time and 2.8 $\times 10^{-13}$ at 10 s gate time. The locking of single comb tooth is achieved by locking the optical comb and the beat note of the CW laser. We used the P(16) overtone transition line of $^{13}C_2H_2$ as the CW reference and optimized the stabilization by choosing appropriate lock point on the Doppler-limited absorption transition. The comb was able to achieve stable locking for almost five hours. The short-term fraction instability of the optical frequency was measured to be 6.56 $\times 10^{-10}$ at 1 s gate time, which is mostly from the CW reference. Our approach of acetylene-stabilized fiber comb offers a feasible solution to help fiber combs move from laboratory to outdoors applications based on fiber sensing, laser stabilization and spectrum analysis.

1. Introduction

In the past two decades, optical frequency comb (OFC) [1–3] has important applications in a wide range of research fields such as optical clock, precision laser spectroscopy, high-accuracy time and frequency transfer, ranging, and lidar [4–9]. More and more outdoor application scenarios require portable OFC with high stability and low cost [10–13]. Fiber-based frequency combs offer many advantages to their free-space counterparts in the aspect of building portable system: common gain media, low-cost semiconductor diode lasers as pump light, all-fiber components avoiding pump misalignment, and oscillator cavities that can be spooled to fit for a compact package. Fiber-based OFCs are reported to serve as a measurement tool for fiber sensing applications, e.g. highly sensitive strain [14] and refractive-index [15] sensing. They can also be used as optical references for laser stabilization and spectrum analysis, for example, in digital holography [16] and breath analysis in medical applications [17].

A fully stabilized OFC relies on the phase stabilization of two degrees of freedom, namely, the carrier-envelope offset frequency (f_{CEO}) and the repetition rate frequency (f_r) [18]. The optical frequency can be expressed in the form of $f_n = f_{CEO} + n \times f_r$, where n is the mode number [2,19,20]. In general, f_r and f_{CEO} are stabilized to an RF reference, e.g. the GPS-disciplined Rb oscillator [21,22]. In this case, the fractional uncertainty of optical frequency is a multiplication of that of the RF standard by the mode number n. Hence, either a high rep rate comb or a high performance RF reference is required such that the multiplied RF instability does not dominate. However, these options are technical challenging and expensive for fiber combs [23,24]. Moreover, the generation of f_{CEO} signals introduces additional complexity and cost of the OFC system [25].

An alternative stabilization scheme is to directly stabilize the OFC to an optical reference, e.g. an ultrastable optical cavity [26,27], a fiber delay line [28], or an atomic or molecular absorption line [29–31]. The high stability of the optical reference can be transferred to other wavelengths through the comb [32,33]. In Ref. [34], Ye et al. used a silicon single crystal optical cavity to reduce thermal noise, leading to a frequency instability of 10^{-16} at 1.5 μm for a Er-doped fiber OFC. In 2019, Ishizawa et al. experimentally demonstrated a narrow-linewidth OFC locked to an ultrastable cavity. The Allan deviation for the in-loop f_{CEO} is 3.3 $\times$ $10^{-16}/\tau$ [35]. Despite the superior OFC stability performance, the system still requires complicated and expensive high finesse cavity. In recent years, Tian et al. reported a CW (continuous wave) laser stabilized to an optical fiber delay line as a reliable and low-cost alternative to optical cavity. The Allan deviation exhibits good short-time stability of 9.13 $\times$ 10^{-13} at 12.8 ms, however, increases to 10^{-11} at 1 s due to the long-term drifting of the referenced fiber delay line [28].

Molecular absorption lines provides long-term stability and absolute accuracy compared to the aforementioned optical references. For

* Corresponding author.
E-mail address: wushun@wit.edu.cn (S. Wu).

https://doi.org/10.1016/j.optcom.2022.129233
Received 12 August 2022; Received in revised form 23 December 2022; Accepted 25 December 2022
Available online 29 December 2022

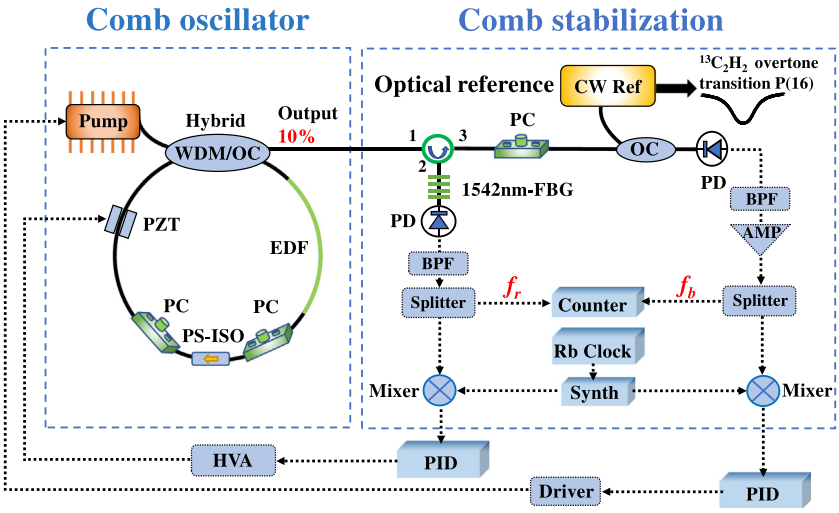

Fig. 1. Schematic diagram of Er-doped fiber optical frequency comb (The black solid line represents the optical signal, and the black dashed line represents the radio frequency signal). WDM: wavelength division multiplexer; PS-ISO: polarization sensitive isolator; EDF: Er-doped fiber; PC: Polarization Controller; PZT: piezoelectric transducer; PD: photodetector; FBG: Fiber Bragg Grating; CW: Continuous Wave; OC: optical coupler; Synth: synthesizer; PID: proportion–integration–differentiation; BPF: band-pass filter; AMP: amplifier; HVA: High voltage amplifier circuit.

1.5 μm radiation, Rb transitions can be used after frequency doubling [29] while Iodine lines can be utilized after frequency tripling [30]. In particular, the acetylene stabilized fiber laser offers a cost effective and reliable solution to a portable comb system with high stability performance. Talvard et al. demonstrated an acetylene-stabilized fiber laser with a sub-kHz short-term linewidth and obtained an Allan deviation below 3×10^{-13} for integration times above 1 s [31]. However, the comb system including the acetylene reference still have a fair share of free-space optical paths. An all-fiber compact and robust OFC system with turn-key operation is required for various outdoor applications. Ref. [36] realized an optically referenced comb system stabilized to an acetylene transition. Knabe et al. utilizes a pump-probe scheme to realize an all-fiber CW reference stabilized to a Doppler-free absorption feature with linewidth of 8 MHz [37]. Both systems were able to achieve fractional stability of 10^{-11} at 1 s gate time, but meanwhile have poor portability due to free-space components including vacuum chambers, Fabry–Perot cavity and etc.

In this paper, we demonstrate an acetylene-referenced all-fiber optical frequency comb and focuses on the stability of the optical frequency. The comb is stabilized to a narrow linewidth CW reference laser referenced to the P(16) line of the v1+v3 acetylene ($^{13}C_2H_2$) overtone transition while the repetition rate (f_r) is locked to the GPS-disciplined Rb oscillator. The standard deviation of f_r in 4.5 hours was 0.37 mHz. The measured fractional stability of f_r is 4.3×10^{-12} at 1 s gate time, and 2.8×10^{-13} at 10 s. We optimized the stability performance for the optical frequency at 1542 nm under various lock-points of the Doppler-limited absorption feature, and achieved a short time stability of 6.56×10^{-10} at 1 s gate time. Our result is similar to Ref. [36,37] but with simpler configurations. When the absorption linewidth is reduced to MHz level, it is expected to realize a frequency stability on the order of 10^{-12}.

Aiming at outdoor applications in fiber sensing and spectrum analysis, this work is a proof-of-principle demonstration of an all-fiber acetylene-stabilized comb system. The comb has a frequency stability that is sufficient for the targeting applications, while being compact and robust with turn-key operation. Some of the existing commercial products, e.g. Toptica and Menlo Systems, have outstanding performance that are beyond the requirement for these applications. Our design can potentially be a good candidate for an inexpensive solution to such application scenarios, in additional to their commercially available counterparts.

2. Experimental setup

Fig. 1 illustrates the schematic of the proposed all-fiber OFC system. The comb oscillator is a home-built femtosecond Er-fiber ring oscillator based on the nonlinear polarization rotation (NPR) mode-locking technique. The 976 nm pump laser was injected into the cavity through a hybrid wavelength-division multiplexer and 10% output coupler (WDM/OC), followed by a 0.38 m Er-doped fiber (EDF; Nufern SM-ESF-7/125) as the gain medium, with the peak absorption of 60 dB/m at 1530 nm. Polarization controllers (PCs) combined with the polarization sensitive isolator (PS-ISO) are used to adjust the polarization state and thus the cavity loss in the oscillator to achieve for a stable mode lock. The length of the ring cavity is 2.05 m. All fibers consisting the cavity have negative dispersion, leading to a total net dispersion of −0.0421 ps^2. Mode-locking is achieved by adjusting the two PCs in the oscillator. The output spectrum is centered at 1560 nm with the full width at half maximum (FWHM) of 14 nm. Fig. 2(a) shows the spectrum measured with a resolution of 0.02 nm by optical spectrum analyzer (OSA, YOKOGAWA, AQ6370C). The laser has a negative close-to-zero net cavity dispersion and operates in the soliton mode locking regime. The output optical spectrum shows a typical soliton-like shape with symmetrical Kelly sidebands. Fig. 2(b) shows the laser output power varying from 2.0 to 3.1 mW as the pump power increases from 160 mW to 280 mW. The laser can self-start mode-locking at pump powers greater than 160 mW, with an output power is 2.3 mW. Fig. 2(c) shows the 97.4 MHz repetition rate observed on the radio frequency spectrum analyzer (RFSA) with a signal-to-noise ratio (SNR) of 68 dB at 300 kHz resolution bandwidth (RBW). The corresponding time interval between adjacent pulses is 10.27 ns on oscilloscope, as shown in Fig. 2(d).

The output of the mode-locked laser goes through the circulator and is split into two paths: the 1542 nm light is reflected by a fiber Bragg grating (FBG) with a 3 dB bandwidth of 0.3 nm and used to perform the heterodyne beat with the CW reference, while the transmitted light from the FBG is utilized for the repetition rate stabilization. The measured rep rate is mixed the reference signal provided by the RF synthesizer. The output of the mixer serves as the error signal for the proportion–integration–differentiation (PID) control. The stabilization of rep rate (f_r) is achieved by sending the feedback control signal to the piezoelectric transducer (PZT) for cavity length control. Meanwhile, the f_{CEO} is frequency-stabilized by locking the RF beatnote (f_b) between the comb and the CW reference, and feeding back to the pump current. All RF signals are referenced to the GPS-disciplined Rb clock in our system.

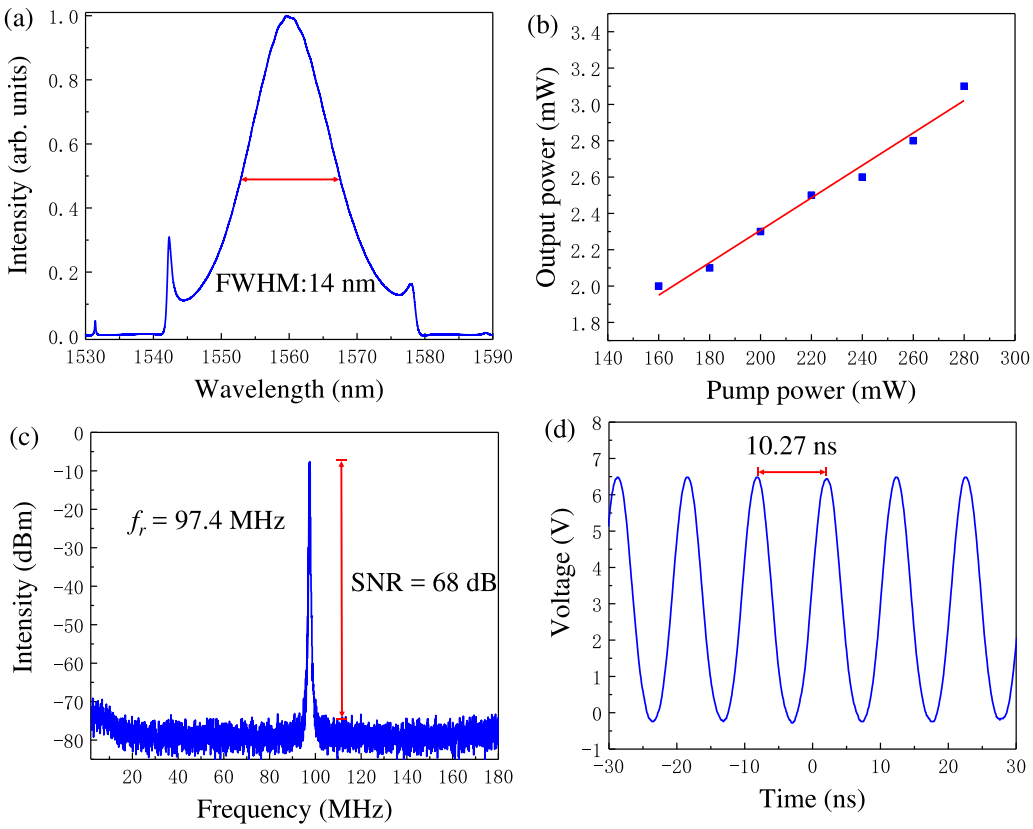

Fig. 2. **(a)** Measured oscillator output spectrum (linear scale) at a pump power of 180 mW. **(b)** The average output power of the oscillator as a function of pump power. **(c)** RF spectrum of the repetition rate. **(d)** Output pulse trains measured by an oscilloscope.

3. Results and discussion

In this section, we discuss the experimental results in three aspects: the stabilization of the CW reference, repetition rate and the optical heterodyne beatnote, respectively.

Fig. 3(a) shows the schematic diagram for the CW reference stabilized to an acetylene gas cell. The laser source is a narrow linewidth fiber laser at 1542 nm with a maximum output power of 35 mW, purchased from NKT Photonics (Model No: Koheras Basik E15). The gas cell is a sealed glass tube, 16.5 cm in length, and filled with 50 Torr acetylene ($^{13}C_2H_2$) gas, purchased from Wavelength References. Both ends of the cell are fiber-coupled with FC/APC interfaces. The optical part of the CW reference is an all-fiber system, with dimensions of 30 × 20×3 cm. As the wavelength of the CW laser was swept at 1 Hz/s triangular wave, we obtained the absorption spectrum of the P(16) line. The transmission light was detected by the photodetector and the converted into an electronic signal, which was further used as the error signal to lock the laser to the molecular transition. To properly characterize the linewidth of the transition, a fiber ring cavity (FRC) was constructed using a 2 × 2 (50:50) fiber coupler. One of the two outputs is connected to one of the two inputs forming a loop. The length of the loop is measured to be 214 cm, corresponding to a free spectral range (FSR) of 93.39 MHz. Fig. 3(b) showed the transmission of the FRC (blue) recorded simultaneously with the absorption signal (black) as the wavelength of the CW laser was swept. The FWHM of the absorption was measured to be 2.2 GHz, as shown in Fig. 3(c).

In order to optimize the lock point of the CW reference, we investigated the locking performance at different lock points with various slopes of the absorption feature, as shown in Fig. 4(a–c). The slopes for lock point A, B and C is calibrated to be 0.138, 0.141 and 0.184 mV/MHz, respectively.

A frequency counter (Keysight 53230A) was used to collect the beatnotes between the CW reference and the comb in three different cases. Fig. 4(a–c) shows the stabilized beatnotes as a function of time for comparison. We can see that at lock point C, which has the largest slope, the CW can be locked for a longer time than that at lock points A and B. The Allan deviations for the three cases are shown in Fig. 4(d). The overall resulting fractional stability for C is about twice better than that in the other two cases. For example, Fig. 4(d) shows an instability of 3.3 × 10^{-10} for C (blue triangle) at 1 s gate time, compared to 6.1 × 10^{-10} for A (black square) and 6.3 × 10^{-10} for B (red dot), respectively. Therefore, we finally chose lock point C for CW reference stabilization, which serves the optical reference for OFC. Further optimization of the locking parameters include the proportional gain, the PI-corner frequency, and the low frequency gain limit (LFGL). In general, using high gain in the electric feedback circuit helps for a long-term robust lock. But if the gain is too high, the system would become unstable and even start oscillating. To investigate how robust the CW reference stabilization is, we measured both the optical response of the laser as well as the servo bandwidth of the feedback loop under various modulation amplitudes. Our results show that the current stabilization is limited to the PZT bandwidth of the laser, which is about 1.5 kHz, while the servo bandwidth is measured to be 4.5 kHz. In addition, our tests also showed that the CW reference remained stable lock when we introduced perturbations such as finger tapping, dropping keychains from above the optical table.

For the repetition rate stabilization, we compared the stability of repetition rate in both unlocked and locked cases, shown in Figs. 5(b) and 5(a), respectively. In the unlocked case, the slow drift of rep rate was mainly caused by the variation in the room temperature. As temperature decreases by 1.3 °C, the cavity length of the oscillator reduces, resulting in an increase in f_r by about 600 Hz. In the locked case, the repetition rate exhibited a standard deviation (SD) of 0.37 mHz for 4.5 hours. For the optical comb tooth stabilization, we combined the filtered comb light reflected from FBG with the CW reference. The optical heterodyne beatnote between the comb and the CW reference was

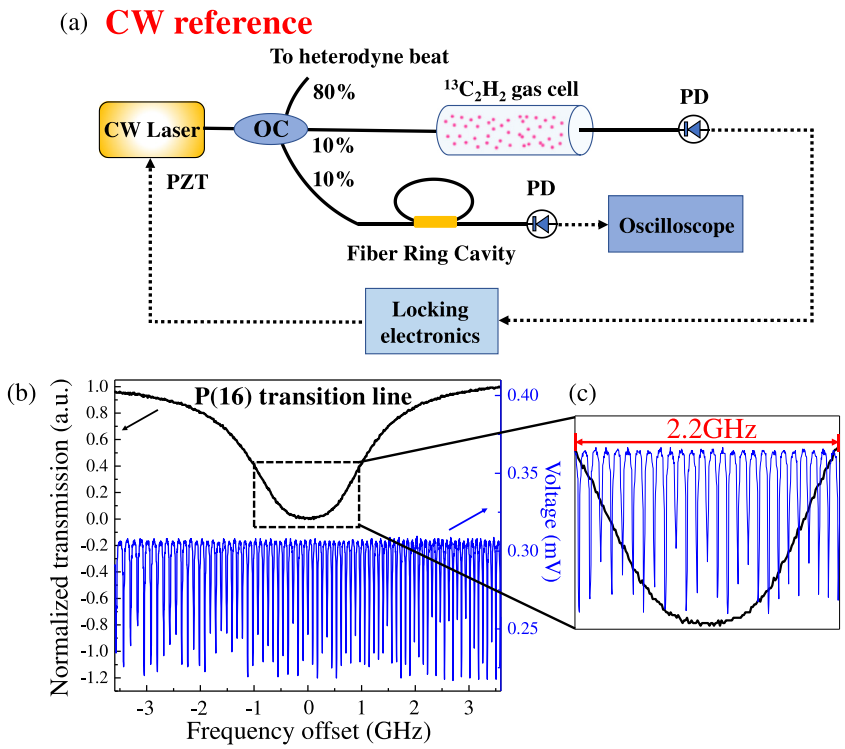

Fig. 3. **(a)** Schematic of the experimental setup for the stabilization of the CW reference. OC: output coupler, PD: photodetector, PZT: piezo transducer. **(b)** The P(16) transition line (black) of $^{13}C_2H_2$ and the transmission spectrum of the FRC (blue). **(c)** The zoom-in picture of the fiber ring cavity, which has a free spectral range of 93.39 MHz, the FWHM of the absorption was measured to be 2.2 GHz.

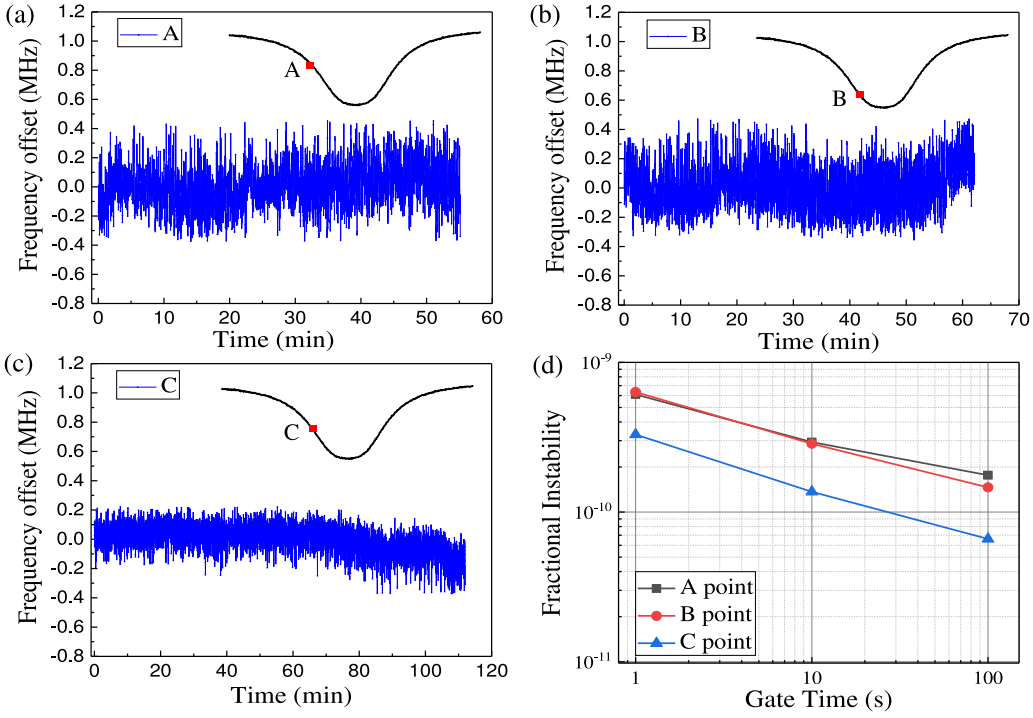

Fig. 4. Comparison of different lock points for the CW reference. **(a–c)** Measured optical heterodyne beatnote between the comb and the CW reference as a function of time when the CW reference is locked to: A (0.138 mV/MHz, Zero reference point: 26.5 MHz), B (0.141 mV/MHz, Zero reference point: 25.8 MHz) and C (0.184 mV/MHz, Zero reference point: 30.4 MHz). **(d)** Calculated fractional instability based on the Allan deviation from **(a–c)**.

detected by a 125 MHz photodetector (Newport 1811). The converted RF beatnote, denoted by f_b, was around 30 MHz. Fig. 6(c) shows the f_b signal with a SNR of 32 dB on the RF spectrum analyzer under 300 kHz RBW. The beatnote was further filtered, amplified and finally mixed with the reference signal from the RF synthesizer, generating the error signal for the following PID control.

The PID control output was fed back to the pump current for the stabilization of f_{CEO}. We recorded the stabilized f_b for 5 hours at a

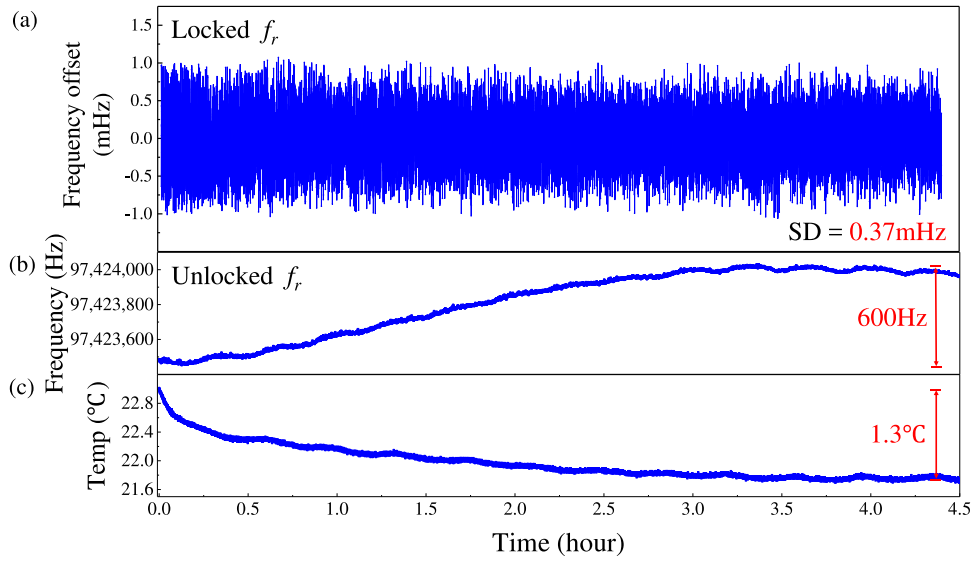

Fig. 5. **(a)** Residual fluctuations of the f_r signal with a 1 s gate. The standard deviation for f_r is 0.37 mHz (Zero reference point: 97.4225587763 MHz). **(b)** Drift variation of repetition rate over 4.5 hours when the optical comb is unlocked. **(c)** Variation of room temperature during the measurement.

gate time of 1 s, as shown in Fig. 6(a). The data shows oscillations with period of about 25 min. This corresponds to the time constant of the temperature control by the air-conditioner in our lab, as displayed in Fig. 6(b).

In addition to optimize the amplification and locking electronics, we also performed instability measurements when both the optical and RF signals were stabilized, as illustrated in Fig. 6. From these measurements, we determined that the instability of the optical frequency at 1542 nm over a period of almost five hours is 6.56×10^{-10} (1 s gate time), represented by the instability of the RF beatnote f_b (black squares).

Meanwhile, the instability of the RF repetition rate from the same measurement, shown in red dots in Fig. 6(d), was found to be 4.3×10^{-12} at 1 s gate time, and 2.8×10^{-13} for a gate time of 10 s. This result is expected to follow the GPS-Rb performance at both short and long time scales. Because all synthesizers and frequency counters were referenced to the GPS-disciplined Rb oscillator in our measurements. However, we can see that only at long time scales, e.g. 10 s, the instability of rep rate approaches to that of the GPS-Rb. We believe that the measurement at short time scales is limited by the performance of the RF synthesizer (RIGOL, Model No. DG4162) used in the experiment. This is verified by the instability test for the RF synthesizer with and without being referenced to the GPS-Rb, as shown in the blue up-triangles and green down-triangles in Fig. 6(d), respectively. The comparison shows that by using GPS-Rb oscillator as the external reference, the stability of the synthesizer did improve by about two orders of magnitude. However, it still cannot fully inherit the stability performance of the GPS-Rb. If replaced by a better synthesizer, the stability of rep rate can approach the GPS-Rb limit.

We performed thorough investigation of our comb system, mainly in three aspects: (a) the bandwidth of the feedback loops, comb stabilization test under (b) various temperatures, and (c) mechanical perturbations. We will discuss the results one by one. Firstly, we measure both the optical response and the closed-loop servo bandwidth for each of the three locking loops. Our results showed that the current locking performance is limited by the CW reference due to the low PZT response of the CW laser. Secondly, in order to investigate how temperature affects the comb behavior, we tested the fractional instability of the optical beatnote as well as the repetition rate under six different environmental temperatures: 18.2, 19.4, 20.5, 21.7, 22.5, and 23.8 °C. The results were quite reproducible: the fractional stability of the beatnote is below 7×10^{-10} while that of the repetition rate is about 4×10^{-12} at 1 s gate time. Temperatures beyond this range cannot be reached due to laboratory conditions. Thirdly, as for the perturbation test, we found that the comb can withstand small perturbations, such as finger tapping the optical table, without degrading the stability performance. Dropping keychains one meter above the laser table would cause the beatnote lockpoint step a few hundred of kHz away but the comb was still capable of maintaining a stable lock afterwards.

According to the comb's equation ($f_n = f_{CEO} + n \times f_r$), the fractional instability of the optical frequency can be expressed as $\Delta f_n/f_n = \Delta f_{CEO}/f_n + n \times \Delta f_r/f_n$, indicating that the instability $\Delta f_n/f_n$ comes from two contributions: the instability of f_{CEO} and f_r. In our case, since the comb's rep rate is about 97 MHz, the mode number n is estimated to be 2×10^6 for wavelength at 1542 nm. Therefore, considering the measured Allan deviation of rep rate is 0.47 mHz, the contribution from f_r instability for 1 s gate time ($n \times \Delta f_r/f_n$) can be calculated as 4×10^{-12}, which is two orders of magnitude better than the current measured short-term stability of the optical frequency (6.56×10^{-10} at 1 s).

Therefore, most contribution of the fractional instability is from the stabilization of the optical comb tooth. Since the stability performance of the CW reference largely depends on the linewidth of the molecular transition, it is important to reduce the molecular linewidth as much as possible. Proposed way to improve the stability of the CW reference include: Firstly, produce a Doppler-free acetylene absorption line by employing the pump–probe technique. Secondly, using a hollow-core fiber with large core size to further reduce the transit-time broadening effect. The short-time stability for a fiber-based acetylene CW reference was reported to be 3×10^{-13} [31]. If integrated in a portable fiber comb system, the comb stability is expected to reach 10^{-12} level, in which case the instability of f_r would become the dominating factor.

4. Conclusions

We have proposed and experimentally demonstrated a compact all-fiber Erbium-doped optical frequency comb based on optical reference. The home-made oscillator is able to achieve self-start mode locking based on the NPR mechanism. The output optical spectrum is centered at 1560 nm and has a FWHM of about 14 nm. The repetition rate f_r stabilization is realized by precise control of the cavity length, while the f_{CEO} is stabilized through locking the RF heterodyne beat between an optical comb tooth and a CW reference. During a time span of almost five hours, the standard deviation of f_r was measured to be

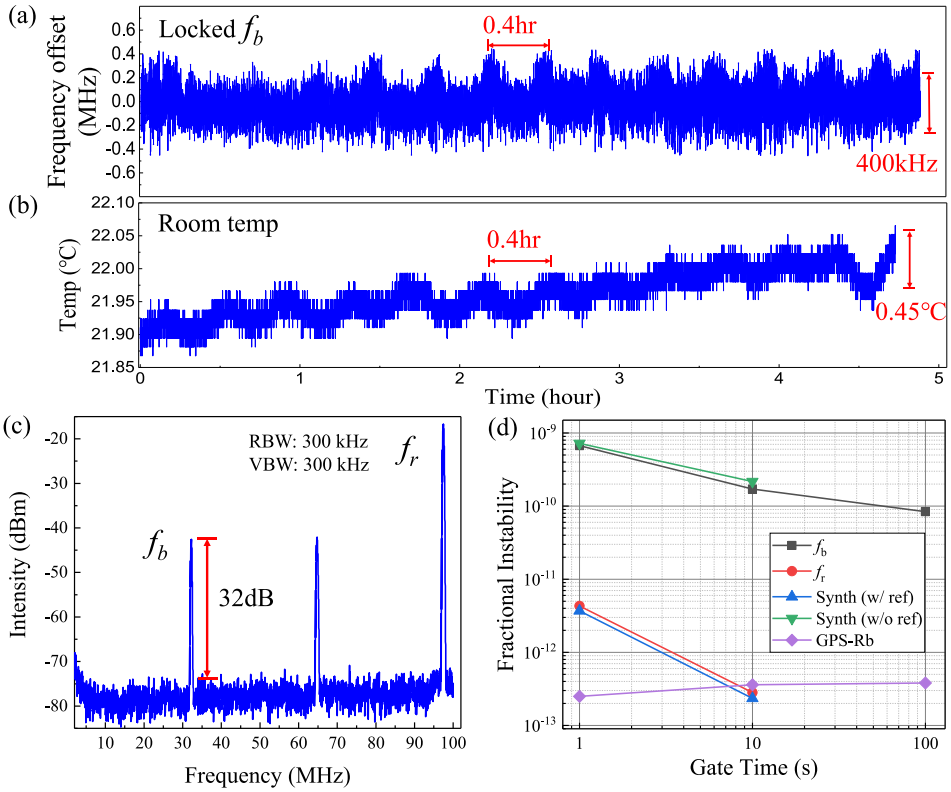

Fig. 6. **(a)** Measured optical heterodyne beatnote between the comb and the CW reference. **(b)** Temperature oscillation in our laboratory when both f_r and f_b are locked simultaneously. **(c)** RF spectrum of the heterodyne beatnote (resolution bandwidth 300 kHz, VBW: video bandwidth). **(d)** Fractional instability of the RF beat between the comb and the CW reference at 1542 nm (black squares) compared to that of the repetition rate (red dots), synthesizer signal with external reference used to lock f_r (blue up-triangles), synthesizer signal without external reference (green down-triangles) and GPS-disciplined Rb oscillator (purple diamonds).

0.37 mHz, resulting in a fractional stability of 4.3×10^{-12} at 1 s gate time, and further down to 2.8×10^{-13} for a gate time of 10 s. We optimized the CW reference stabilization by trying different lock points from the Doppler-limited absorption line at 1542 nm. Our results show that the fractional instability of the optical frequency is measured to be 6.56×10^{-10} at 1 s gate time, which is a dominating contribution to the fractional stability of the comb.

Compared to a PM fiber laser, e.g. SESAM-based laser, our low-cost homemade NPR laser covers the 1542 nm wavelength component without additional amplification. The optical heterodyne beating process involves the comb light directly from the oscillator, rather than after optical amplification, which avoids introducing excessive noise and ensures a beatnote with high signal-to-noise ratio (>30 dB). This is essential for achieving a stable comb performance.

A possible upgrade of the system would be to employ the pump–probe technique and obtain a Doppler-free absorption feature for the $^{13}C_2H_2$ P(16) line, which can reduce the linewidth by three orders of magnitude and leading to a short-time stability performance on the order of 10^{-12} for an all-fiber portable comb system. Additional temperature control module can be implemented which shields the system from external temperature changes. With reliable performance and all-fiber design for a compact comb system, we are targeting at outdoor applications in the field of laser stabilization and fiber sensing, which demands for medium cost with high portability. Our approach of acetylene-stabilized fiber comb provides a simple and inexpensive solution for an optical frequency reference, as an alternative choice compared to some over-cost commercial products.

Declaration of competing interest

The authors declare that they have no known competing financial interests or personal relationships that could have appeared to influence the work reported in this paper.

Data availability

No data was used for the research described in the article.

Acknowledgments

This work is supported by grants from Campus Science Foundation of Wuhan Institute of Technology, China [22QD01], and Open Research Fund of State Key Laboratory of Transient Optics and Photonics, China [SKLST202105], and Graduate Innovative Fund of Wuhan Institute of Technology, China [NO. CX2021385].

References

[1] N. Picqué, T.W. Hänsch, Frequency comb spectroscopy, Nat. Photon. 13 (2019) 146–157.
[2] J. Kim, Y. Song, Ultralow-noise mode-locked fiber lasers and frequency combs: principles, status, and applications, Adv. Opt. Photon. 8 (2016) 465.
[3] S.A. Diddams, The evolving optical frequency comb [Invited], J. Opt. Soc. Am. B. 27 (2010) 51.
[4] M.J. Thorpe, D. Balslev-Clausen, M.S. Kirchner, J. Ye, Cavity-enhanced optical frequency comb spectroscopy: application to human breath analysis, Opt. Express. 16 (2008) 2387.
[5] D. Pile, Transparent nanofibre paper, Nat. Photon. 3 (2009) 314.
[6] T. Fortier, E. Baumann, 20 Years of developments in optical frequency comb technology and applications, Commun. Phys. 2 (2019) 153.
[7] N.R. Newbury, Searching for applications with a fine-tooth comb, Nat. Photon. 5 (2011) 186.
[8] D.I. Herman, C. Weerasekara, L.C. Hutcherson, F.R. Giorgetta, K.C. Cossel, E.M. Waxman, G.M. Colacion, N.R. Newbury, S.M. Welch, B.D. DePaola, I. Coddington, E.A. Santos, B.R. Washburn, Precise multispecies agricultural gas flux determined using broadband open-path dual-comb spectroscopy, Sci. Adv. 7 (2021) 9765.
[9] Z. Deng, Y. Liu, Z. Zhu, D. Luo, C. Gu, Z. Zuo, G. Xie, W. Li, Achieving precise spectral analysis and imaging simultaneously with a mode-resolved dual-comb interferometer, Sensors. 21 (2021) 3166.

[10] G.B. Rieker, F.R. Giorgetta, W.C. Swann, J. Kofler, A.M. Zolot, L.C. Sinclair, E. Baumann, C. Cromer, G. Petron, C. Sweeney, P.P. Tans, I. Coddington, N.R. Newbury, Frequency-comb-based remote sensing of greenhouse gases over kilometer air paths, Optica. 1 (2014) 290.
[11] L.C. Sinclair, I. Coddington, W.C. Swann, G.B. Rieker, A. Hati, K. Iwakuni, N.R. Newbury, Operation of an optically coherent frequency comb outside the metrology lab, Opt. Express. 22 (2014) 6996.
[12] L.C. Sinclair, J.-D. Deschênes, L. Sonderhouse, W.C. Swann, I.H. Khader, E. Baumann, N.R. Newbury, I. Coddington, Invited article: A compact optically coherent fiber frequency comb, Rev. Sci. Instrum. 86 (2015) 081301.
[13] C. Lee, S.T. Chu, B.E. Little, J. Bland-Hawthorn, S. Leon-Saval, Portable frequency combs for optical frequency metrology, Opt. Express. 20 (2012) 16671.
[14] T. Minamikawa, T. Ogura, Y. Nakajima, Y. Mizutani, H. Yamamoto, T. Yasui, Strain sensing based on strain to radio- frequency conversion of an optical frequency comb, Opt. Express. 26 (2018) 9484.
[15] R. Oe, S. Taue, T. Minamikawa, K. Nagai, K. Shibuya, T. Mizuno, M. Yamagiwa, Y. Mizutani, H. Yamamoto, T. Iwata, H. Fukano, Y. Nakajima, K. Minoshima, T. Yasui, Refractive-index-sensing optical comb based on photonic radio-frequency conversion with intracavity multi-mode interference fiber sensor, Opt. Express. 26 (2018) 19694.
[16] M. Yamagiwa, T. Minamikawa, C. Trovato, T. Ogawa, D.G.A. Ibrahim, Y. Kawahito, R. Oe, K. Shibuya, T. Mizuno, E. Abraham, Y. Mizutani, T. Iwata, H. Yamamoto, K. Minoshima, T. Yasui, Multicascade-linked synthetic wavelength digital holography using an optical-comb-referenced frequency synthesizer, Opt. Express. 26 (2018) 26292.
[17] M.J. Thorpe, D. Balslev-Clausen, M.S. Kirchner, J. Ye, Cavity-enhanced optical frequency comb spectroscopy: application to human breath analysis, Opt. Express. 16 (2008) 2387.
[18] H. Inaba, Y. Daimon, F.-L. Hong, A. Onae, K. Minoshima, T.R. Schibli, H. Matsumoto, M. Hirano, T. Okuno, M. Onishi, M. Nakazawa, Long-term measurement of optical frequencies using a simple, robust and low-noise fiber based frequency comb, Opt. Express 14 (2006) 5223.
[19] T. Udem, R. Holzwarth, T.W. Hänsch, Optical Frequency Metrology. 416, 2002, p. 5.
[20] S. Droste, G. Ycas, B.R. Washburn, I. Coddington, N.R. Newbury, Optical frequency comb generation based on erbium fiber lasers, Nanophotonics 5 (2016) 196–213.
[21] J.A. Stone, P. Egan, An optical frequency comb tied to GPS for laser frequency/wavelength calibration, J. Res. Natl. Inst. Stand. Technol. 115 (2010) 413.
[22] H. Wu, T. Ma, Q. Lu, J. Ma, L. Shi, Q. Mao, Optical frequency combs based on a period-doubling mode-locked Er-doped fiber laser, Opt. Express. 26 (2018) 577.
[23] G. Xie, Y. Liu, L. Zhou, Z. Zhu, Z. Deng, D. Luo, C. Gu, W. Li, Self-referenced frequency comb from a polarization-maintaining Er: Fiber laser based nonlinear polarization evolution, Results Phys. 22 (2021) 103886.
[24] Y. Li, N. Kuse, A. Rolland, Y. Stepanenko, C. Radzewicz, M.E. Fermann, Low noise, self-referenced all polarization maintaining ytterbium fiber laser frequency comb, Opt. Express. 25 (2017) 18017.
[25] Y. Feng, X. Xu, X. Hu, Y. Liu, Y. Wang, W. Zhang, Z. Yang, L. Duan, W. Zhao, Z. Cheng, Environmental-adaptability analysis of an all polarization-maintaining fiber-based optical frequency comb, Opt. Express. 23 (2015) 17549.
[26] R.W.P. Drever, J.L. Hall, F.V. Kowalski, J. Hough, G.M. Ford, A.J. Munley, H. Ward, Laser phase and frequency stabilization using an optical resonator, Appl. Phys. B. 31 (1983) 97–105.
[27] H. Yang, S. Zhang, W. Zhao, L. Zhang, Coherent narrow-linewidth optical frequency synthesis across the optical telecommunication band, Appl. Opt. 59 (2020) 4865.
[28] H. Tian, F. Meng, K. Wang, B. Lin, S. Cao, Z. Fang, Y. Song, M. Hu, Optical frequency comb stabilized to a fiber delay line, Appl. Phys. Lett. 119 (2021) 121106.
[29] H.S. Moon, H.Y. Ryu, S.H. Lee, H.S. Suh, Precision spectroscopy of Rb atoms using single comb-line selected from fiber optical frequency comb, Opt. Express. 19 (2011) 15855.
[30] C. Philippe, R. Le Targat, D. Holleville, M. Lours, Tuan. Minh-Pham, J. Hrabina, F. Du Burck, P. Wolf, O. Acef, Frequency tripled 1.5μm telecom laser diode stabilized to iodine hyperfine line in the 10^{-15} range, in: 2016 European Frequency and Time Forum, EFTF, IEEE, York, 2016, pp. 1–3.
[31] T. Talvard, P.G. Westergaard, M.V. DePalatis, N.F. Mortensen, M. Drewsen, B. Gøth, J. Hald, Enhancement of the performance of a fiber-based frequency comb by referencing to an acetylene-stabilized fiber laser, Opt. Express. 25 (2017) 2259.
[32] D. Nicolodi, B. Argence, W. Zhang, R. Le Targat, G. Santarelli, Y. Le Coq, Spectral purity transfer between optical wavelengths at the 10^{-18} level, Nat. Photonics. 8 (2014) 219–223.
[33] L. Pang, H. Han, Z. Zhao, W. Liu, Z. Wei, Ultra-stability Yb-doped fiber optical frequency comb with 2×10^{-18}/s stability in-loop, Opt. Express. 24 (2016) 28993.
[34] T. Kessler, C. Hagemann, C. Grebing, T. Legero, U. Sterr, F. Riehle, M.J. Martin, L. Chen, J. Ye, A sub-40 mHz linewidth laser based on a silicon single-crystal optical cavity, Nat. Photon. 6 (2012) 687–692.
[35] A. Ishizawa, K. Hitomi, K. Hara, K. Hitachi, T. Nishikawa, T. Sogawa, H. Gotoh, Simple method for stabilizing an optical frequency comb to an optical reference without an RF signal generator, OSA Continuum. 2 (2019) 1706.
[36] S. Wu, C. Wang, C. Fourcade-Dutin, B.R. Washburn, F. Benabid, K.L. Corwin, Direct fiber comb stabilization to a gas-filled hollow-core photonic crystal fiber, Opt. Express. 22 (2014) 23704.
[37] K. Knabe, S. Wu, J. Lim, K.A. Tillman, P.S. Light, F. Couny, N. Wheeler, R. Thapa, A.M. Jones, J.W. Nicholson, B.R. Washburn, F. Benabid, K.L. Corwin, 10 kHz accuracy of an optical frequency reference based on $^{12}C_2H_2$-filled large-core kagome photonic crystal fibers, Opt. Express. 17 (2009) 16017.